Narrowing in the differences of urban and non-urban surface ozone levels in summers of the Northern Hemisphere

Han Han[1], Lin Zhang[1,*], Zehui Liu[1], Xu Yue[2], Lei Shu[3], Yuanhang Zhang[4,*]

[1]Laboratory for Climate and Ocean-Atmosphere Studies, Department of Atmospheric and Oceanic Sciences, School of Physics, Peking University, Beijing 100871, China

[2]Jiangsu Key Laboratory of Atmospheric Environment Monitoring and Pollution Control, Collaborative Innovation Center of Atmospheric Environment and Equipment Technology, School of Environmental Science and Engineering, Nanjing University of Information Science & Technology, Nanjing 210044, China

[3]School of Environmental Science and Engineering, Southern University of Science and Technology, Shenzhen 518055, China

[4]State Key Joint Laboratory of Environmental Simulation and Pollution Control, College of Environmental Sciences and Engineering, Peking University, Beijing 100871, China

Correspondence to: Lin Zhang (zhanglg@pku.edu.cn) and Yuanhang Zhang (yhzhang@pku.edu.cn)

Key points

- Global pairs of urban and non-urban ozone observation sites are constructed.
- Urban vs. non-urban ozone differences have substantially narrowed in summers of many Northern mid-latitude regions over 1990–2020.
- Anthropogenic emission controls of nitrogen oxides have led to closer ozone formation regimes at the urban and non-urban areas.

Abstract

Differences of surface ozone levels between urban and non-urban areas provide a good indicator of local ozone formation regimes. However, trends in the urban vs. non-urban ozone differences over the past decades are unclear. Here, we construct 6361 pairs of urban and non-urban ozone measurement sites to assess the trends worldwide. We find that urban vs. non-urban ozone differences have greatly narrowed in the summers of Northern mid-latitude countries over 1990–2020. Analyses of satellite measurements of ozone precursors and statistical predictions driven by meteorology show that, the reduction in anthropogenic emissions of nitrogen oxides, which weakened the titration of ozone over urban areas, is probably the dominant driver of the narrowing difference. Climate change partly contributes to the narrowing trend. Our results indicate that surface ozone concentrations and ozone formation regimes become increasingly similar over urban and non-urban areas, and this shall be considered in future air pollution controls.

Key words: ozone, urban-rural difference, air pollution, nitrogen oxides, ozone trend

Plain language summary

Surface ozone is a key air pollutant affecting human and vegetation health and its levels may differ largely over urban and non-urban areas. In the traditional view, surface ozone concentrations were found to be lower over urban than nearby non-urban areas, which can be explained by higher anthropogenic emissions of nitrogen oxides and thus stronger titration of ozone over urban areas. In the past decades, global emissions of ozone precursors have changed substantially. However, trends in the urban vs. non-urban ozone differences are still unknown. Here, we find that urban vs. non-urban ozone differences have greatly narrowed in summers of North America, Europe, Korea, and Japan over 1990–2020 and even narrowed to nearly zero over some cities. We demonstrate that the narrowing difference is dominantly driven by the anthropogenic emission control of nitrogen oxides, which weakened the titration of ozone over urban areas and led to similar ozone formation conditions over urban and non-urban areas. Climate change also slightly contributes to the narrowing trend at some cities, such as Berlin and Tokyo. The narrowing ozone differences between urban and non-urban areas indicate that future air pollution control policies shall also pay attention to non-urban areas.

1. Introduction

Surface ozone is a major air pollutant that harms human health and ecosystems (Feng et al., 2019; Jerrett et al., 2009; Turner et al., 2016). It is mainly produced from the photochemical oxidation of volatile organic compounds (VOCs) and carbon monoxide (CO) in the presence of nitrogen oxides (NO_x). Countries across the world, especially in North America, Europe, and East Asia, have established nationwide observational networks to monitor ozone air quality (Cooper et al., 2014; Wang et al., 2017). Using these observations, the recent Tropospheric Ozone Assessment Report (TOAR) showed that surface ozone concentrations declined significantly in eastern North America and Europe from 2000 to 2014, and meanwhile increased notably in South Korea and Japan (Chang et al., 2017; Lefohn et al., 2018). Starting in 2013, China greatly expanded the ozone observation network, from which the observed surface ozone levels over most Chinese sites have shown rapid increases during 2013–2019 (Lu et al., 2020).

Surface ozone and its environmental effects may differ greatly over urban and non-urban areas because of different anthropogenic activities, meteorological conditions, and ecological environment (Jaffe et al., 2007; P. Li et al., 2018; Sillman et al., 1999). Urban vs. non-urban ozone differences reflect the non-linear sensitivity of ozone formation to local emissions of its precursors. As found in Europe and North America, surface ozone concentrations tended to be lower over urban than nearby non-urban areas, which can be explained by higher anthropogenic NO_x emissions and thus stronger titration of ozone over urban areas (Akimoto et al., 2015; Derwent & Hjellbrekke, 2013; Paoletti et al., 2014; Zhang et al., 2004). Recently, Gao et al. (2020) reported lower ozone concentrations over urban than suburban areas in Beijing-Tianjin-Hebei of China in 2015–2018. In the past decades, emissions of ozone precursors have changed substantially over the globe (Hoesly et al., 2018). Although Fleming et al. (2018) using five quantitative ozone metrics relevant for human exposure suggested that the trends of urban and non-urban ozone in North America and Europe were broadly similar during 2000–2014, how the urban vs. non-urban

ozone differences evolve under the emission changes is unclear. In this study, using observations from the China National Environmental Monitoring Center (CNEMC), the United States (US) Environmental Protection Agency (EPA), European Environment Agency (EEA) and TOAR, we will present a global comparison of ozone concentrations and trends between the urban and non-urban areas during 1990–2020.

Surface ozone trend is determined by both anthropogenic and non-anthropogenic processes (Wilson et al., 2012). Reductions in anthropogenic emissions drove a negative trend in surface ozone over the eastern US during 1991–2010 (Cooper et al., 2012; Strode et al., 2015). Emission controls in Europe also lowered the peak ozone concentrations during 1995–2014 (Yan et al., 2018). Meteorology can impact surface ozone trends by altering natural emissions of ozone precursors (Lin et al., 2017), ozone chemical production and loss (Andersson et al., 2007), atmospheric transport (Nagashima et al., 2017), and dry deposition (Lin et al., 2020). Recent studies suggested that surface ozone increases over some regions in China during 2013–2017 induced by meteorological variability could have an equal or even greater importance than emission changes (M. Li et al., 2021; Liu & Wang, 2020). Here, using a generalized multiple linear regression (GMLR) model driven by meteorological variables that are highly correlated with surface ozone variability, we will further diagnose the anthropogenic and meteorological contributions to the surface ozone trend with a focus on the urban vs. non-urban ozone differences.

2. Data and methods

2.1. Surface ozone observations

Surface ozone measurements from TOAR covering the globe 1990–2014 (Schultz et al., 2017a, b; https://toar-data.org/surface-data/), CNEMC covering China 2013–2020 (https://quotsoft.net/air/), EPA covering the US 2013–2020 (https://aqs.epa.gov/aqsweb/airdata/download_files.html), and EEA covering Europe 2013–2020 (https://www.eea.europa.eu/data-and-maps/data/aqereporting-9) were used

in this study. The measurements were combined over the TOAR and CNEMC observation sites (Text S1). By matching the locations of the observation sites, ozone data from EPA and EEA were used to expand the temporal coverage of the observations over the TOAR sites in the US and Europe to 2020. We calculated the daily maximum 8-hour average (MDA8) ozone at each TOAR and CNEMC observation site at each day, and focused on monthly mean MDA8 ozone concentrations in boreal summer (June–August). Only measurements from the sites with at least 6-year continuous June–August monthly records were used (Text S1). We then selected 5258 sites out of 11679 total monitoring sites. Trends in surface ozone were calculated by the slopes of the linear regression (Text S1) and were reported with *p* values. Following the recommendation of the American Statistical Association (Wasserstein et al., 2019), we do not treat $p<0.05$ as a 'bright-line' of statistically significance or meaningful (Chang et al., 2020; Cooper et al., 2020; Tarasick et al., 2019; Gaudel et al., 2019).

2.2. Classification of paired urban and non-urban sites

We constructed global urban-suburban and urban-rural pairs of ozone observation sites to examine the urban vs. non-urban ozone differences and their trends in each city. First, we identified the urban and non-urban sites in the ozone datasets used in this study by adopting the classification method in TOAR (Schultz et al., 2017a). A site was classified as an urban site when it met the following criteria: (1) the population density ≥ 1000 people km^{-2}, (2) nighttime lights within a 25 km radius of the monitoring site reach the maxima of the brightness index (set as the value of 63 in the light dataset) (3) nighttime lights at the observation site ≥ 60. Using the classification approach (Table S1), we classified 1568 out of 5258 sites as urban sites over the globe, 385 out of 1703 sites in North America, 307 of 1619 sites in Europe, 824 of 1810 sites in East Asia, 366 of 839 sites in China, and 454 of 959 sites in Korea and Japan (Table S2).

For each urban site, we paired the site with a suburban site that was located

within a 50 km radius of the urban site, and also paired a rural site with a searching distance of 100 km. Finally, we mapped 4152 urban-suburban and 2209 urban-rural pairs over the globe based on the classified 1568 urban, 813 suburban, and 624 rural sites (Figure S1). Regionally, there were 329 urban-suburban and 441 urban-rural pairs in North America, 1374 and 1099 pairs in Europe, 2444 and 342 pairs in East Asia, 165 and 9 pairs in China, and 2279 and 333 pairs in Korea and Japan (Table S2). Some urban sites may pair with more than one non-urban sites, while some may not pair with any non-urban site. The population and nighttime light datasets used in the classification are described in Text S2.

Satellite observations of formaldehyde (HCHO) total column and nitrogen dioxide (NO_2) tropospheric column were used to identify the ozone formation regimes for both urban and non-urban sites in the study. The datasets were retrieved by the Ozone Monitoring Instrument (OMI) and acquired from NASA's Goddard Earth Sciences Data and Information Services Center (GES DISC) (https://earthdata.nasa.gov/eosdis/sips/omi-sips). The level-3 daily HCHO and NO_2 products have a horizontal resolution of 0.1° latitude ×0.1° longitude and 0.25° latitude×0.25° longitude, respectively, with global coverage since 2005. Here the daily HCHO and NO_2 column observations were sampled over each ozone monitoring site at their resolutions.

2.3. Anthropogenic and meteorological contributions to surface ozone trend

We developed a GMLR model to quantify the contributions of changes in meteorology and climate to the surface ozone trend at each observation site (Gong et al., 2021; K. Li et al., 2019; Ziemke et al., 2019). We first applied a stepwise multiple linear regression to evaluate the correlations between daily MDA8 ozone and 7 meteorological variables, including temperature at 2 m, relative humidity at 2 m, total cloud cover, total precipitation, zonal wind at 850 hPa, meridional wind at 850 hPa, and wind speed at 850 hPa. Previous studies have reported significant linear relationships among them in North America (Porter et al., 2015), Europe (Otero et al.,

2016), and China (Han et al., 2020). Here, we further identified that the ozone-meteorology linear regression slopes correlate with meteorological variables, which reflects a quadratic relationship between them (Fu et al., 2015). For example, Figure S2 shows strong correlations between ozone-temperature regression slopes and meteorology using the sites with at least 15-year continuous observations. Such strong correlations indicate that surface ozone is highly correlated with the square term of temperature and the product of temperature and relative humidity (Pusede et al., 2015).

Therefore, our GMLR model accounts for the squared terms for each predictor and products of predictors as described by Equation (1):

$$\hat{Y} = b + \sum_{i=1}^{7} \alpha_i X_i + \sum_{i=1}^{7} \beta_i X_i^2 + \sum_{i=1}^{7} \sum_{j=i}^{7} \gamma_{i,j} X_i X_j \qquad (1)$$

where $\hat{Y}$ is the predicted value of surface ozone, b is the intercept term, X_i and X_j are the meteorological variables, and α_i, β_i, and $\gamma_{i,j}$ are regression coefficients. We performed the GMLR at each observation site. The leave-one-out cross validation was used to avoid overfitting (Han et al., 2020). The resulting GMLR explains 20%–40% daily variations of surface ozone in North America, 40%–70% in Europe, and 30%–40% in East Asia. Trend in the predicted ozone values can be then interpreted as the contribution of changes in meteorology or climate to the observed trend. Trend in the residual is estimated as that driven by non-meteorological conditions. In most situations, it is also termed as anthropogenic contribution to the surface ozone trend (K. Li et al, 2019). Differences in the contributions of anthropogenic or meteorological factors to the ozone trend between urban and non-urban areas are used to represent their contributions to the trends in urban vs. non-urban ozone differences. Here we used the meteorological data from the ERA5 reanalysis data (https://www.ecmwf.int/en/forecasts/datasets/reanalysis-datasets/era5) produced by the European Centre for Medium-Range Weather Forecasts (ECMWF) available on 0.25° latitude × 0.25° longitude resolution.

3. Results and discussion

3.1. Differences of urban and non-urban ozone levels and their trends in North America, Europe, Korea, and Japan

Figure 1 compares the surface MDA8 ozone concentrations among urban, suburban, and rural areas in North America, Europe, and East Asia in boreal summer. Values are calculated over 2013–2020 in China and over 2000–2014 in the other regions. Surface ozone levels tend to be lower at urban areas than suburban and rural areas in North America and Europe, with some exceptions, e.g., in the Southeast US where urban ozone levels are higher than rural ozone. Regional mean ozone levels are the lowest at urban areas and the highest at rural areas in North America, Europe, Korea, and Japan. Regional mean urban ozone levels are higher than suburban levels for the paired sites in China, which will be discussed in Section 3.3. By analyzing the ozone trends (Figure S3), we can see that MDA8 ozone levels over urban, suburban, and rural areas have all decreased substantially in North America and Europe from 2000 to 2014, while weaker trends can be seen over urban than suburban and rural areas. On the contrast, surface MDA8 ozone concentrations have increased in Korea and Japan over 2000–2014, with stronger trends over urban than suburban and rural areas (Figure S3). Such trends in surface ozone indicate that the differences among urban, suburban, and rural ozone over these regions have narrowed from 2000 to 2014.

Narrowing of the ozone differences is a robust feature when extending the time period to 1990s–2010s. Figure 2 shows that the urban vs. suburban and urban vs. rural summer mean ozone differences in North America, Europe, Korea, and Japan have narrowed on decadal scale from 1990 to 2020. Urban vs. suburban and urban vs. rural MDA8 ozone differences respectively narrowed from 3.0 to 0.2 ppbv and from 4.3 to 0.8 ppbv in North America. In Europe, urban MDA8 ozone increased slightly from 1990s to 2010s. This is consistent with the results in Lu et al. (2018), which identified weak trends in seasonal mean MDA8 ozone while decreasing trends in other ozone exposure metrics, including 4MDA8, NDGT70, and AOT40 in Europe over 1990–

2014. The urban vs. suburban and urban vs. rural MDA8 ozone differences in Europe respectively narrowed from 3.9 to 1.4 ppbv and from 9.0 to 4.2 ppbv from 1990s to 2010s. In Korea and Japan, regional mean urban MDA8 ozone increased by 6.0 ppbv from 1990s to 2010s while the urban vs. suburban differences narrowed from 4.2 to 0.7 ppbv.

3.2. Drivers of the trends in the differences of urban and non-urban ozone levels in North America, Europe, Korea, and Japan

Using the GMLR, we separate the contributions from climate and anthropogenic changes to the trends in the differences of urban vs. non-urban ozone levels. Changes in anthropogenic sources show dominant contributions to the narrowing differences over 1990–2020 with varying contributions from changes in climate. The GMLR model predicts small climatic effects on the 1990–2020 inter-decadal changes of regional mean ozone over the northern mid-latitude regions, except for Europe, where the climatic contributed trend in the urban vs. non-urban ozone differences is distinct (Figure 2).

Here we examine the urban-suburban and urban-rural ozone differences at 14 representative cities worldwide, as shown in Figures 3 and S4, including three cities in North America, four in Europe, six in East Asia, and one in Australia. Most of the cities show narrowing of the urban vs. non-urban ozone differences except of the cities in China as will be discussed in the next section. We use the satellite observed HCHO over NO_2 column ratios (FNR) to further identify the anthropogenic drivers of the narrowing differences. We define the contrast of FNR (CFNR) as the ratio of urban vs. non-urban FNR, so that CFNR values of close to 1 indicate similar ozone formation regimes over urban and non-urban areas. Figure 4 shows the results over four cities and additional cities are shown in Figures S5–S6.

Based on the trends of urban MDA8 ozone, we categorize the cities with narrowing differences of urban and non-urban ozone into two groups: one group with

decreasing trend or slight changes in urban MDA8 ozone and one group with increasing trend in urban MDA8 ozone. The first group includes Los Angeles, Montreal, Boston, and Zurich, and the second group includes Berlin, Madrid, and Tokyo (Figure 3). In Los Angeles of the US, urban vs. rural MDA8 ozone differences narrowed at a rate of 0.91 ppbv yr^{-1} from 2001 to 2015 (Figure S4). HCHO columns increased over both urban and rural areas from 2005 to 2020, while NO_2 tropospheric columns over Los Angeles city decreased at a rate of 2.6 times stronger than that over its rural areas from 2005 to 2020. Similar features can be seen in other cities of the first group. Effective emission controls have been implemented in these cities, in particular reducing NO_x emissions and ambient levels and thus weakening the ozone titration in urban areas. The urban vs. non-urban contrasts in the NO_x concentration have been narrowed, leading to more closer ozone formation regimes as evidenced by the trend of CFNR in Figure 4.

For the second group, e.g., in Berlin of Germany, urban MDA8 ozone concentrations increased at 0.53 ppbv yr^{-1} from 1990 to 2020, with comparable contributions from changes in climate (51%) and anthropogenic sources (49%). Increase in surface air temperature, decrease in surface humidity, and decrease in wind speed are likely the key climatic factors for the urban ozone increase in Berlin (Table S3). In Madrid of Spain, urban MDA8 ozone concentrations increased remarkably (0.99 ppbv yr^{-1}) from 1997 to 2011, associated with rapid decreases in NO_2 columns and small changes in HCHO columns over 2005–2020 (Figure S5). These ozone increases were likely attributed to anthropogenic NO_x emission reductions under the VOC-limited ozone formation regime (Querol et al., 2016). Urban MDA8 ozone concentrations have also increased in Seoul and Tokyo in recent years (Figure 3). In spite of surface ozone increases over these cities, narrowing of urban vs. non-urban differences can be seen, with changes in climate contribute 3%-29% of the narrowing (Figure S4). The dominant driving factor can also be attributed to the rapid declines of NO_x emissions in urban areas, which have narrowed urban vs. non-urban NO_2 column differences while changes in HCHO columns are

indistinguishable.

3.3. Differences of urban and non-urban ozone levels in China

We now analyze the recent ozone increases in China over 2013–2020 from the urban vs. non-urban perspective. China was observed as a global hot spot of present-day surface ozone pollution with greater human and vegetation exposure than other developed regions of the world (Lu et al., 2018). Figure S3 shows that the national mean surface MDA8 ozone concentrations at both urban and suburban sites have increased greatly from 2013 to 2020, with rates of 2.59 and 2.55 ppbv yr^{-1}, respectively. Over some areas, the surface MDA8 ozone increasing rate reaches as high as ~6.0 ppbv yr^{-1} (Figure S7). In the North China Plain (114°E–119°E, 36°N–40°N), where the ozone levels are high (Figure 1), urban MDA8 ozone increased by 21.8 ppbv from 2013 to 2020. Applying the GMLR, we estimate that anthropogenic and meteorological factors respectively contribute to 57% and 43% of the ozone increase over paired urban sites in the North China Plain. The results are consistent with previous studies (K. Li et al., 2019; M. Li et al., 2021), emphasizing the important role of meteorological changes. We also identify that surface MDA8 ozone increased at most of the rural sites in China over 2013–2020, which is contributed by both anthropogenic and meteorological factors (Figures S3 and S7).

For paired urban and non-urban sites, the ozone differences in China are more mixed than in North America, Europe, Korea, and Japan (Figure 1). Urban MDA8 ozone levels are higher than suburban levels at 56% of the Chinese urban-suburban pairs in summer 2013–2020, leading to a national mean difference of 1.7±2.8 (50% of the standard deviation) ppbv. Only 9 urban-rural pairs are identified in China, and we find lower urban MDA8 ozone than rural ozone, with a mean difference of −4.8±3.0 ppbv. Figure 3 compares the urban and non-urban ozone at the four Chinese cities: Beijing, Guangzhou, Hangzhou, and Lanzhou. Urban minus suburban MDA8 ozone differences are, respectively, 3.5±3.2, 1.4±2.0, 5.1±3.0, and 4.2±4.9 ppbv in the four cities (Table S4). None obvious trends in the urban vs. suburban and urban vs. rural

ozone differences have been observed at these cities over 2013–2020, except for Lanzhou (Figures 3 and S4). However, in two cities (Beijing and Guangzhou), there are observational evidence that the urban vs. non-urban NO_2 column differences have narrowed with insignificant changes in the HCHO column differences, leading to closer ozone formation regimes over their urban and suburban areas (Figure 4 and Figure S6). The strong surface ozone increases over different station types of area indicate that ozone air pollution shows an increasing regional-scale feature, and both urban and non-urban areas require attention in mitigating the severe ozone pollution in China.

4. Summary

Based on datasets from TOAR, CNEMC, EPA, and EEA, we have constructed 4152 urban-suburban and 2209 urban-rural pairs of ozone measurement sites from the selected 1568 urban, 813 suburban, and 624 rural sites. We find that urban ozone tends to be lower than suburban and rural ozone in Northern Hemispheric developing regions, and their differences have substantially narrowed over 1990–2020. We demonstrate that the narrowing differences are dominantly driven by the decreases of anthropogenic NO_x emissions. The reduction in NO_x weakened its titration of ozone over urban areas, and led to closer formation regimes in cities and their surrounding non-urban areas. Changes in climate also partly drive the narrowing differences in some cities, such as Berlin and Tokyo. Urban vs. suburban ozone differences in China over 2013–2020 suggests no clear changes while ozone formation regimes over some urban and non-urban areas also become close. More non-urban observation sites are called in the future expansion of the ozone observation network in China. As surface ozone concentrations and formation regimes become similar over urban and non-urban areas, future air pollution control measures shall pay increasing attention to non-urban ozone levels and broader regional scales.

Acknowledgements

The authors gratefully acknowledge the TOAR initiative for providing the ozone data

collection. OMI HCHO and NO_2 data were acquired from NASA's GES DISC. Population, nighttime lights, and meteorological data were, respectively, acquired from the SEDAC at Columbia University, NOAA EOG, and ECMWF. We thank Dr. Owen R. Cooper at NOAA Chemical Sciences Laboratory for useful suggestions on data analysis. The research is supported by the National Natural Science Foundation of China (41922037) and China Postdoctoral Science Foundation (2021M690002).

Conflict of interest

The authors declare that they have no competing financial interest.

Data availability statement

Ozone data from TOAR, CNEMC, EPA, EEA can be accessed from https://toar-data.org/surface-data/, https://quotsoft.net/air/, https://aqs.epa.gov/aqsweb/airdata/download_files.html, https://www.eea.europa.eu/data-and-maps/data/aqereporting-9, respectively. Population data from the SEDAC at Columbia University and MDSP-OLS nighttime lights data can be respectively downloaded from https://sedac.ciesin.columbia.edu/data/set/gpw-v4-population-density-rev11/data-download and https://ngdc.noaa.gov/eog/dmsp/downloadV4composites.html. OMI HCHO and NO_2 products from NASA's GES DISC can be acquired from https://earthdata.nasa.gov/eosdis/sips/omi-sips. The ERA5 meteorological reanalysis data can be downloaded from https://www.ecmwf.int/en/forecasts/datasets/reanalysis-datasets/era5.

Supporting Information

References

Akimoto, H., Mori, Y., Sasaki, K., Nakanishi, H., Ohizumi, T., & Itano, Y. (2015). Analysis of monitoring data of ground-level ozone in Japan for long-term trend during 1990–2010: Causes of temporal and spatial variation. Atmospheric Environment, 102, 302–310, https://doi.org/10.1016/j.atmosenv.2014.12.001.

Andersson, C., Langner, J., & Bergstrom, R. (2007). Interannual variation and trends in air pollution over Europe due to climate variability during 1958–2001 simulated with a regional CTM coupled to the ERA40 reanalysis. Tellus B: Chemical and Physical Meteorology, 59 (1), 77–98. https://doi.org/10.1111/j.1600-0889.2006.00231.x.

Chang, K. L., Cooper, O. R., Gaudel, A., Petropavlovskikh, I., & Thouret, V. (2020). Statistical regularization for trend detection: an integrated approach for detecting long-term trends from sparse tropospheric ozone profiles. Atmospheric Chemistry and Physics, 20 (16), 9915–9938. https://doi.org/10.5194/acp-20-9915-2020.

Chang, K.-L., Petropavlovskikh, I., Copper, O. R., Schultz, M. G., & Wang, T. (2017). Regional trend analysis of surface ozone observations from monitoring networks in eastern North America, Europe and East Asia. Elementa: Science of the Anthropocene, 5, 50. https://doi.org/10.1525/elementa.243.

Cooper, O. R., Gao, R. S., Tarasick, D., Leblanc, T., & Sweeney, C. (2012). Long-term ozone trends at rural ozone monitoring sites across the United States, 1990–2010. Journal of Geophysical Research, 117, D22307. https://doi.org/10.1029/2012JD018261.

Cooper, O. R., Parrish, D. D., Ziemke, J., Balashov, N. V., Cupeiro, M., Galbally, I. E., Gilge, S., Horowitz, L., Jensen, N. R., Lamarque, J. -F., Naik, V., Oltmans, S. J., Schwab, J., Shindell, D. T., Thompson, A. M., Thouret, V., Wang, Y., & Zbinden, R. M. (2014). Global distribution and trends of tropospheric ozone: An observation-based review. Elementa: Science of the Anthropocene, 2, 29. https://doi.org/10.12952/journal.elementa.000029.

Cooper, O. R., Schultz, M. G., Schroder, S., Chang, K. L., Gaudel, A., Benitez, G. C., Cuevas, E., Frohlich, M., Galbally, I. E., Molloy, S., Kubistin, D., Lu, X., McClure-Begley, A., Nedelec, P., O'Brien, J., Oltmans, S. J., Petropavlovskikh, I., Ries, L., Senik, I., Sjoberg, K., Solberg, S., Spain, G. T., Spangl, W., Steinbacher, M., Tarasick, D., Thouret, V., & Xu, X. (2020). Multi-decadal surface ozone trends at globally distributed remote locations. Elementa: Science of the Anthropocene, 8, 23. https://doi.org/10.1525/elementa.420.

Derwent, R. G., & Hjellbrekke, A.-G. (2013). Air Pollution by Ozone Across Europe, Urban Air Quality in Europe, edited by: Viana, M., Springer. https://doi.org/10.1007/698_2012_163.

Feng, Z., De Marco, A., Anav, A., Gualtieri, M., Sicard, P., Tian, H., Fornasier, F., Tao, F., Guo, A., & Paoletti, E. (2019). Economic losses due to ozone impacts on human health, forest productivity and crop yield across China. Environmental International, 131, 104966. https://doi.org/10.1016/j.envint.2019.104966.

Fleming, Z. L., Doherty, R. M., Von Schneidemesser, E., Malley, C. S., Cooper, O. R., Pinto, J. P., Colette, A., Xu, X., Simpson, D., Schultz, M. G., Lefohn, A. S.,

Hamad, S., Moolla, R., Solberg, S., & Feng, Z. (2018). Tropospheric Ozone Assessment Report: Present-day ozone distribution and trends relevant to human health. Elementa: Science of the Anthropocene, 6, 12. https://doi.org/10.1525/elementa.273.

Fu, T., Zheng, Y., Paulot, F., Mao, J., & Yantosca, R. M. (2015). Positive but variable sensitivity of August surface ozone to large-scale warming in the southeast United States. Nature Climate Change, 5 (5), 454–458. https://doi.org/10.1038/NCLIMATE2567.

Gao, L., Yue, X., Meng, X., Du, L., Lei, Y., Tian, C., & Qiu, L. (2020). Comparison of Ozone and $PM_{2.5}$ Concentrations over Urban, Suburban, and Background Sites in China. Advances in Atmospheric Sciences, 37 (12), 1297–1309. https://doi.org/10.1007/s00376-020-0054-2.

Gaudel, A., Cooper, O. R., Chang, K. L., Bourgeois, I., Ziemke, J. R., Strode, S. A., Oman, L. D., Sellitto, P., Nedelec, P., Blot, R., Thouret, V., & Granier, C. (2020). Aircraft observations since the 1990s reveal increases of tropospheric ozone at multiple locations across the Northern Hemisphere. Science Advances, 6 (34), eaba8272. https://doi.org/10.1126/sciadv.aba8272.

Gong, S., Liu, H., Zhang, B., He, J., Zhang, H., Wang, Y., Wang, S., Zhang, L., & Wang, J. (2021). Assessment of meteorology vs. control measures in the China fine particular matter trend from 2013 to 2019 by an environmental meteorology index. Atmospheric Chemistry and Physics, 21 (4), 2999–3013. https://doi.org/10.5194/acp-21-2999-2021.

Han, H., Liu, J., Shu, L., Wang, T., & Yuan, H. (2020). Local and synoptic meteorological influences on daily variability in summertime surface ozone in eastern China. Atmospheric Chemistry and Physics, 20 (1), 203–222. https://doi.org/10.5194/acp-20-203-2020.

Hoesly, R. M., Smith, S. J., Feng, L., Klimont, Z., Janssens-Maenhout, G., Pitkanen, T., Seibert, J. J., Vu, L., Andres, R. J., Bolt, R. M., Bond, T. C., Dawidowski, L., Kholod, N., Kurokawa, J.-I., Li, M., Liu, L., Lu, Z., Moura, M. C. P., O'Rourke, P. R., and Zhang, Q. (2018). Historical (1750–2014) anthropogenic emissions of reactive gases and aerosols from the Community Emissions Data System (CEDS). Geoscientific Model Devolopment, 11, 369–408. https://doi.org/10.5194/gmd-11-369-2018.

Jaffe, D. & Ray, J. (2007). Increase in surface ozone at rural sites in the western US. Atmospheric Environment, 41 (26), 5452–5463. https://doi.org/10.1016/j.atmosenv.2007.02.034.

Jerrett, M., Burnett, R. T., Pope, C. A., Ito, K., Thurston, G., Krewski, D., Shi, Y. L., Calle, E., & Thun, M. (2009). Long-Term Ozone Exposure and Mortality. New England Journal of Medicine, 360 (11), 1085–1095. https://doi.org/10.1056/NEJMoa0803894.

Lefohn, A. S., Malley, C. S., Smith, L., Wells, B., Hazucha, M., Simon, H., Naik, V., Mills, G., Schultz, M. G., Paoletti, E., De Marco, A., Xu, X., Zhang, L., Wang, T., Neufeld, H. S., Musselman, R. C., Tarasick, D., Brauer, M., Feng, Z., Tang, H., Kobayashi, K., Sicard, P., Solberg, S., & Gerosa, G. (2018). Tropospheric ozone

assessment report: Global ozone metrics for climate change, human health, and crop/ecosystem research. Elementa: Science of the Anthropocene, 6, 28. https://doi.org/10.1525/elementa.279.

Li, K., Jacob, D. J., Liao, H., Shen, L., Zhang, Q., & Bates, K. H. (2019). Anthropogenic drivers of 2013–2017 trends in summer surface ozone in China. Proceedings of the National Academy of Sciences of the United States of America, 116, 422–427. https://doi.org/10.1073/pnas.1812168116.

Li, M., Wang, T., Shu, L., Qu, Y., Xie, M., Liu, J., Wu, H., & Kalsoom, U. (2021). Rising surface ozone in China from 2013 to 2017: A response to the recent atmospheric warming or pollutant controls? Atmospheric Environment, 246, 118130. https://doi.org/10.1016/j.atmosenv.2020.118130.

Li, P., De Marco, A., Feng, Z., Anav, A., Zhou, D. & Paoletti, E. (2018). Nationwide ground-level ozone measurements in China suggest serious risks to forests. Environmental Pollution, 237, 803–813. https://doi.org/10.1016/j.envpol.2017.11.002.

Lin, M., Horowitz, L. W., Payton, R., Fiore, A. M., & Tonnesen, G. (2017). US surface ozone trends and extremes from 1980 to 2014: quantifying the roles of rising Asian emissions, domestic controls, wildfires, and climate. Atmospheric Chemistry and Physics, 17 (4), 2943–2970. https://doi.org/10.5194/acp-17-2943-2017.

Lin, M., Horowitz, L. W., Xie, Y., Paulot, F., Malyshev, S., Shevliakova, E., Finco, A., Gerosa, G., Kubistin, D., & Pilegaard, K. (2020). Vegetation feedbacks during drought exacerbate ozone air pollution extremes in Europe. Nature Climate Change, 10 (5), 444–451. https://doi.org/10.1038/s41558-020-0743-y.

Liu, Y. & Wang, T. (2020). Worsening urban ozone pollution in China from 2013 to 2017 – Part 2: The effects of emission changes and implications for multi-pollutant control. Atmospheric Chemistry and Physics, 20 (11), 6323–6337. https://doi.org/10.5194/acp-20-6323-2020.

Lu, X., Hong, J., Zhang, L., Cooper, O. R., Schultz, M. G., Xu, X., Wang, T., Gao, M., Zhao, Y., & Zhang, Y. (2018). Severe Surface Ozone Pollution in China: A Global Perspective. Environmental Science & Technology Letters, 5 (8), 487–494. https://doi.org/10.1021/acs.estlett.8b00366.

Lu, X., Zhang, L., Wang, X., Gao, M., Li, K., Zhang, Y., Yue, X., & Zhang, Y. (2020). Rapid Increases in Warm-Season Surface Ozone and Resulting Health Impact in China Since 2013. Environmental Science & Technology Letters, 7 (4), 240–247. https://doi.org/10.1021/acs.estlett.0c00171.

Nagashima, T., Sudo, K., Akimoto, H., Kurokawa, J., & Ohara, T. (2017). Long-term change in the source contribution to surface ozone over Japan. Atmospheric Chemistry and Physics, 17 (13), 8231–8246. https://doi.org/10.5194/acp-17-8231-2017.

Otero, N., Sillmann, J., Schnell, J. L., Rust, H. W., & Butler, T. (2016). Synoptic and meteorological drivers of extreme ozone concentrations over Europe. Environmental Research Letter, 11 (2), 024005. https://doi.org/10.1088/1748-9326/11/2/024005.

Paoletti, E., De Marco, A., Beddows, D. C. S., Harrison, R. M., & Manning, W. J. (2014). Ozone levels in European and USA cities are increasing more than at rural sites, while peak values are decreasing. Environmental Pollution, 2014, 192, 295–299. http://dx.doi.org/10.1016/j.envpol.2014.04.040.

Porter, W. C., Heald, C. L., Cooley, D., & Russell, B. (2015). Investigating the observed sensitivities of air-quality extremes to meteorological drivers via quantile regression. Atmospheric Chemistry and Physics, 15 (18), 10349–10366. https://doi.org/10.5194/acp-15-10349-2015.

Pusede, S. E., Steiner, A. L., & Cohen, R. C. (2015). Temperature and Recent Trends in the Chemistry of Continental Surface Ozone. Chemical Reviews, 115 (10), 3898–3918. https://doi.org/10.1021/cr5006815.

Querol, X., Alastuey, A., Reche, C., Orio, A., Pallares, M., Reina, F., Dieguez, J. J., Mantilla, E., Escudero, M., Alonso, L., Gangoiti, G., & Millan, M. (2016). On the origin of the highest ozone episodes in Spain. Science of the Total Environment, 572, 379–389. http://dx.doi.org/10.1016/j.scitotenv.2016.07.193.

Schultz, M. G., Schröder, S., Lyapina, O., Cooper, O., Galbally, I., Petropavlovskikh, I., Von Schneidemesser, E., Tanimoto, H., Elshorbany, Y., Naja, M., Seguel, R., Dauert, U. et al. (2017a). Tropospheric Ozone Assessment Report: Database and Metrics Data of Global Surface Ozone Observations. Elementa: Science of the Anthropocene, 5, 58. https://doi.org/10.1525/elementa.244.

Schultz, M. G., Schroder, S., Lyapina, O., Cooper, O., Galbally, I., Petropavlovskikh, I., Von Schneidemesser, E., Tanimoto, H., Elshorbany, Y., Naja, M., Seguel, R., Dauert, U. et al. (2017b). Tropospheric Ozone Assessment Report, links to Global surface ozone datasets. PANGAEA. https://doi.org/10.1594/PANGAEA.876108.

Sillman, S. (1999). The relation between ozone, NO_x and hydrocarbons in urban and polluted rural environments. Atmospheric Environment, 33 (12), 1821–1845. https://doi.org/10.1016/S1352-2310(98)00345-8.

Strode, S. A., Rodriguez, J. M., Logan, J. A., Cooper, O. R., Witte, J. C., Lamsal, L. N., Damon, M., Van Aartsen, B., Steenrod, S. D., & Strahan, S. E. (2015). Trends and variability in surface ozone over the United States. Journal of Geophysical Research, 120 (7), 9020–9042. https://doi.org/10.1002/2014JD022784.

Tarasick, D., Galbally, I. E., Cooper, O. R., Schultz, M. G., Ancellet, G., Leblanc, T., Wallington, T. J., Ziemke, J., Liu, X., Steinbacher, M., Staehelin, J., Vigouroux, C., Hannigan, J. W., Garcia, O., Foret, G., Zanis, P., Weatherhead, E., Petropavlovskikh, I., Worden, H., Osman, M., Liu, J., Chang, K. L., Gaudel, A., Lin, M. Y., Granados-Munoz, M., Thompson, A. M., Oltmans, S. J., Cuesta, J., Dufour, G., Thouret, V., Hassler, B., Trickl, T., & Neu, J. L. (2019). Tropospheric Ozone Assessment Report: Tropospheric ozone from 1877 to 2016, observed levels, trends and uncertainties. Elementa: Science of the Anthropocene, 7, 39. https://doi.org/10.1525/elementa.376.

Turner, M. C., Jerrett, M., Pope, C. A., Krewski, D., Gapstur, S. M., Diver, W. R., Beckerman, B. S., Marshall, J. D., Su, J., Crouse, D. L., & Burnett, R. T. (2016). Long-Term Ozone Exposure and Mortality in a Large Prospective Study. American Journal of Respiratory and Critical Care Medicine, 193 (10), 1134–1142.

https://doi.org/10.1164/rccm.201508-1633OC.

Wang, T., Xue, L., Brimblecombe, P., Lam, Y. F., Li, L., & Zhang, L. (2017). Ozone pollution in China: A review of concentrations, meteorological influences, chemical precursors, and effects. Science of the Total Environment, 2017, 575, 1582–1596. https://doi.org/10.1016/j.scitotenv.2016.10.081.

Wasserstein, R. L., Schirm, A. L., & Lazar, N. A. (2019). Moving to a world beyond p < 0.05. The American Statistician, 73, 1–29. https://doi.org/10.1080/00031305.2019.1583913.

Wilson, R. C., Fleming, Z. L., Monks, P. S., Clain, G., Henne, S., Konovalov, I. B., Szopa, S., & Menut, L. (2012). Have primary emission reduction measures reduced ozone across Europe? An analysis of European rural background ozone trends 1996–2005. Atmospheric Chemistry and Physics, 12 (1), 437–454. https://doi.org/10.5194/acp-12-437-2012.

Yan, Y., Pozzer, A., Ojha, N., Lin, J., & Lelieveld, J. (2018). Analysis of European ozone trends in the period 1995-2014. Atmospheric Chemistry and Physics, 18 (8), 5589–5605. https://doi.org/10.5194/acp-18-5589-2018.

Zhang, R., Lei, W., Tie, X., & Hess, P. (2004). Industrial emissions cause extreme urban ozone diurnal variability. Proceedings of the National Academy of Sciences of the United States of America, 101 (17), 6346–6350, https://doi.org/10.1073/pnas.0401484101.

Ziemke, J. R., Oman, L. D., Strode, S. A., Douglass, A. R., Olsen, M. A., McPeters, R. D., Bhartia, P. K., Froidevaux, L., Labow, G. J., Witte, J. C., Thompson, A. M., Haffner, D. P., Kramarova, N. A., Frith, S. M., Huang, L.-K., Jaross, G. R., Seftor, C. J., Deland, M. T., & Taylor, S. L. (2019). Trends in global tropospheric ozone inferred from a composite record of TOMS/OMI/MLS/OMPS satellite measurements and the MERRA-2 GMI simulation, Atmospheric Chemistry and Physics, 19 (5), 3257–3269. https://doi.org/10.5194/acp-19-3257-2019.

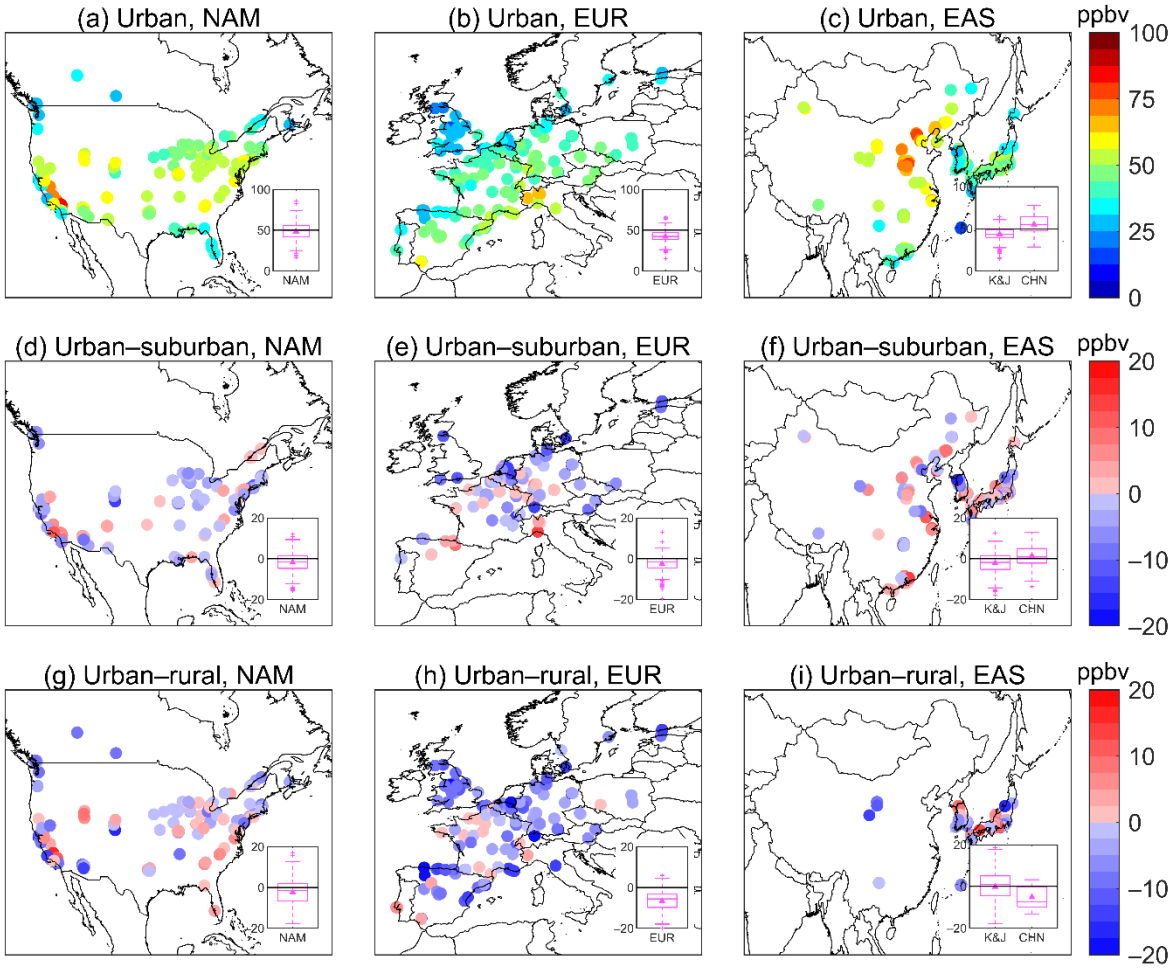

Figure 1. Urban MDA8 ozone concentrations in North America (NAM), Europe (EUR), and East Asia (EAS) (a–c), and their differences with suburban (d–f) and rural (g–i) areas in boreal summer. The concentrations are averaged over 2000–2014 in North America, Europe, and Korea and Japan (K&J), and over 2013–2020 in China (CHN). Box-whisker plots (25th percentile, median, 75th percentile, and lines above/below the box denote 95th/5th percentiles) with triangles indicating the regional means are shown inset.

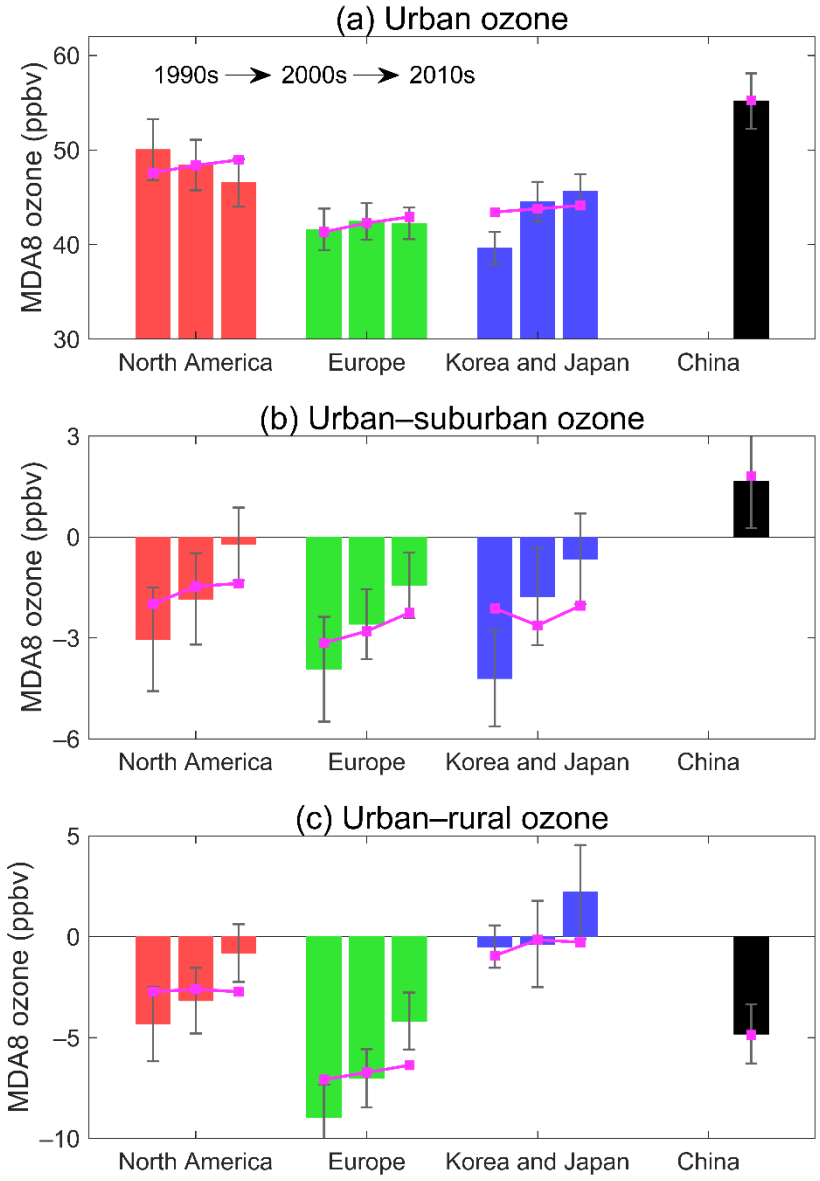

Figure 2. Inter-decadal changes of urban MDA8 ozone (a), MDA8 ozone differences between urban and suburban areas (b), and MDA8 ozone differences between urban and rural areas (c) in boreal summer from 1990 to 2020. The three bars for each region indicate the values calculated from the available observation period in each decade (Table S2). The error bars are ±25% the standard deviation for the observation sites in each region. The purple lines connect the values predicted by the GMLR model.

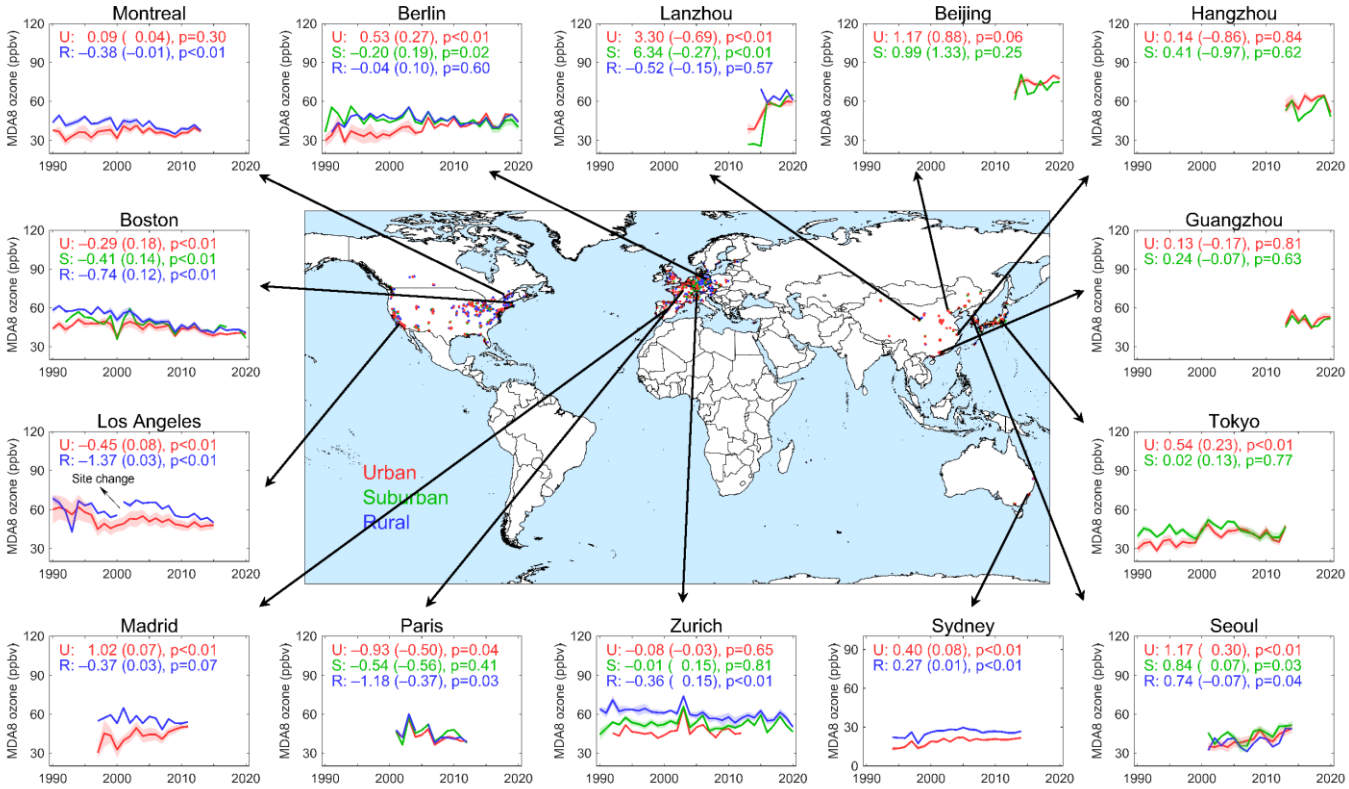

Figure 3. Global comparison of surface MDA8 ozone concentrations and trends (ppbv yr^{-1}) over urban (U, in red), suburban (S, in green) and rural (R, in blue) areas in boreal summer. The central panel shows global distribution of the paired sites, and is surrounded by time series of ozone concentrations at 14 cities worldwide. The number of sites and available observation period are shown in Table S2. The shaded areas represent the standard deviations among the corresponding sites for each city. Numbers in the brackets show contributions of changes in climate to the ozone trends as estimated by the GMLR model. The trends over Los Angeles are calculated over 2001–2015.

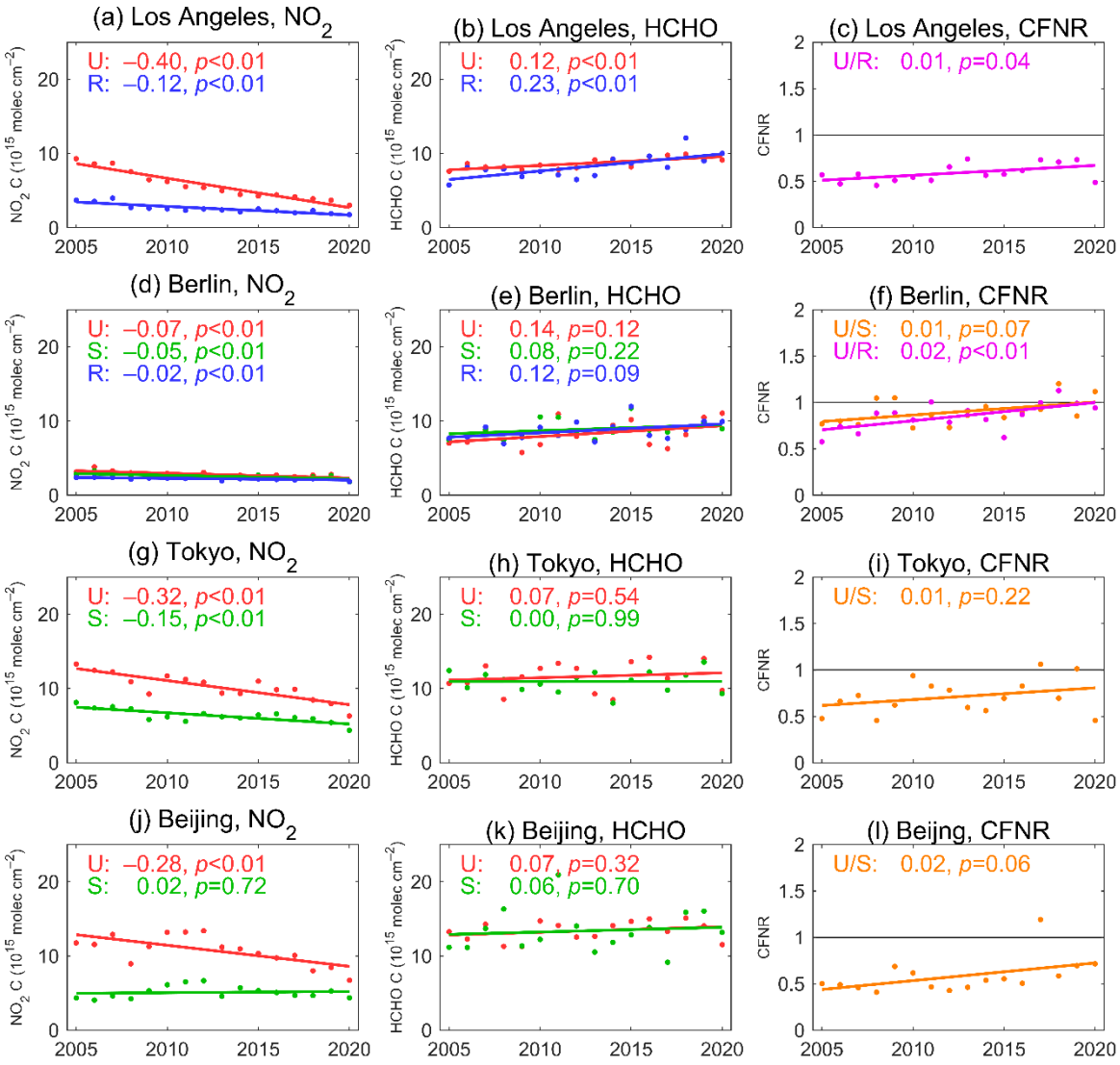

Figure 4. OMI observed boreal summer mean NO_2 tropospheric columns (left panels), HCHO columns (middle panels), and urban vs. non-urban contrasts of $HCHO/NO_2$ ratios (CFNR, right panels) in four cities worldwide (Los Angeles, Berlin, Tokyo, and Beijing) from 2005 to 2020. Linear regression lines are shown for urban (U) in red, suburban (S) in green, and rural (R) in green, urban vs. suburban (U/S) CFNR in orange, and urban vs. rural (U/R) CFNR in purple. The linear regression slopes and *p* values are shown inset.